

## Strategies for the synthesis of porous metal phosphonate materials†

Gary B. Hix,<sup>\*a</sup> Adele Turner,<sup>a</sup> Benson M. Kariuki,<sup>b</sup> Maryjane Tremayne<sup>b</sup> and Elizabeth J. MacLean<sup>c</sup><sup>a</sup>Department of Chemistry, De Montfort University, The Gateway, Leicester, UK LE1 9BH.  
E-mail: ghix@dmu.ac.uk; Fax: 0116 257 7135<sup>b</sup>School of Chemical Sciences, University of Birmingham, Edgbaston, Birmingham, UK B15 2TT<sup>c</sup>CLRC Daresbury Laboratory, Daresbury, Warrington, Cheshire, UK WA4 4AD

Received 29th April 2002, Accepted 18th June 2002

First published as an Advance Article on the web 3rd October 2002

The use of bifunctional phosphonate anions and metal cations that can adopt different co-ordination environments is proposed as a strategy for synthesising porous metal phosphonates. The hydrothermal methods described use phosphonic acids and dialkylphosphonates, which are hydrolysed *in situ* by the acidic metal solutions, to derive the desired phosphonate anions. A series of isostructural hydroxymethylphosphonates,  $M(O_3PCH_2OH)$  [ $M = Zn, Co, Cu$  and  $Mn$ ], which contain a hexagonal array of cylindrical channels (approximate diameter 5.7 Å), were prepared by reaction of the relevant metal acetate with diethyl hydroxymethylphosphonate.  $Zn(O_3PCH_2C(O)NH_2) \cdot H_2O$  was prepared by reaction of zinc acetate and diethyl cyanomethylphosphonate. The structure was determined by single crystal X-ray diffraction and contains two orthogonal channel systems with water molecules situated at the intersections of the channels.  $Zn_3(O_3PCH_2CO_2)_2 \cdot nH_2O$  [ $n = 3, 4$ ] was prepared by reaction of phosphonoacetic acid and zinc acetate. Single crystal analysis reveals the presence of channels in the [100] direction with a cross-section of  $10.02 \times 6.78$  Å. All three of the Zn-based materials can be isomorphously doped with Co.

## Introduction

Metal phosphonates (materials containing  $O_3PR$  groups, where R is an organic functional group) were first reported around 25 years ago by Yamanaka *et al.*<sup>1</sup> Since then, much effort has been put into the synthesis and chemistry of these materials, and has resulted in the development of new synthetic methods and strategies. The aim of this paper is to review some of these, and to present the methods and strategies currently employed in our laboratory, within the context of porous metal phosphonates.

Yamanaka's work, based on that of Clearfield and Smith<sup>2</sup> and Alberti *et al.*<sup>3</sup> on layered zirconium hydrogen phosphates, proved to be the first of thousands of papers that would be published on the subject of layered  $M(IV)$  phosphonates. The structure of these materials can briefly be described as an inorganic layer, consisting of  $M(IV)$  ions octahedrally co-ordinated by  $PO_3$  groups, with the organic functional group pendant in the interlayer region (shown schematically in Fig. 1). There is now an enormous diversity in the organic functional groups that can be included in these materials. Early work was concerned with simple phosphonates,<sup>4</sup> where R is an alkyl chain or phenyl group, whereas later studies have involved more complex groups, *e.g.* crown ethers, viologens and bipyridyls.<sup>5</sup>

The majority of these layered materials have a common method of synthesis, regardless of the functional group. The procedure involves the initial formation of a fluoride complex of the  $M(IV)$  cation in solution, which is subsequently decomposed at 60–70 °C in the presence of a phosphonic acid. The attraction of this method is its general applicability to the synthesis of a large number of different materials with a wide range of organic functional groups.

Attempts to synthesise porous  $M(IV)$  phosphonates have largely been based upon the inclusion of biphosphonate anions,

$[O_3P-R-PO_3]^{4-}$ .<sup>6</sup> In  $M(IV)$  phosphonates, these anions effectively form a bridge between two metal atoms. However, the resulting materials are often not porous due to the bulk of the R group. With few exceptions, attempts to induce porosity by interspersing smaller phosphate or phosphite groups between the pillars are reported to give rise to mesoporosity due to structural disorder. At best, the porosity is not uniform and broad pore size distributions are observed. Results from our own work suggest that the rates of reaction between metal and phosphonic acids vary with the functional group.<sup>7</sup>

The syntheses of  $M(II)$  [and  $M(III)$ ] derivatives are diverse in nature (unlike  $M(IV)$  phosphonates), and often depend upon the nature of the organic group and the metal being used. This was demonstrated by the work of Cunningham *et al.* in 1979,<sup>8</sup> in which a number of simple reactions between metal salts and phosphonic acids were considered, with the product being formed simply as a precipitate. In several cases, he was unable

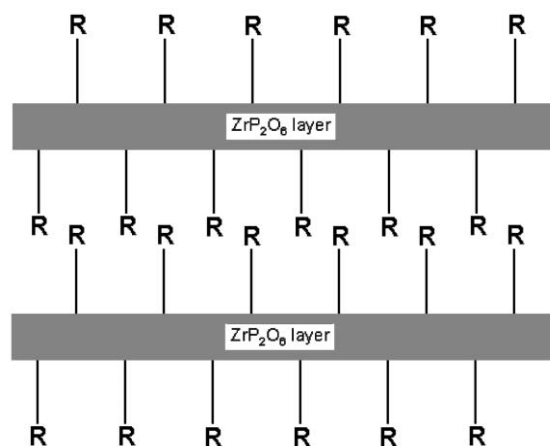


Fig. 1 Schematic representation of the arrangement of layers in zirconium phosphonates.

†Basis of a presentation given at Materials Discussion No. 5, 22–25 September 2002, Madrid, Spain.

to obtain a precipitate when using an acid, and could only obtain a solid product by using a mono- or disodium salt of the acid. In other cases, precipitation of the product would only occur if the reaction mixture was refluxed. In addition, different materials can be formed from the same metal and phosphonate group depending upon the synthetic conditions employed, as shown by Bruque *et al.* in 1998.<sup>9</sup> In this paper, six different aluminium phenylphosphonates were synthesised by varying the reagents (*e.g.* different Al salts) used and the reaction conditions (*e.g.* reflux or hydrothermal). Other workers have shown that, when hydrothermal methods are employed, variation of the reaction temperature, the pH of the reaction mixture, the absolute and relative concentrations of reactants and the nature of the metal salt can lead to a number of different phases being formed from the same metal and phosphonate.<sup>9,10</sup>

The main synthetic method currently employed in the synthesis of phosphonate materials is the use of hydro- or solvothermal reactions. Besides the major benefit of providing sizeable single crystals of many materials, this approach has led to the synthesis of a number of products that are not formed by direct precipitation.

Another synthetic approach is the reaction of molten phosphonic acids with inorganic salts of the required metal. This method has been shown to be particularly successful in the synthesis of nickel,<sup>11</sup> copper<sup>12</sup> and aluminium phosphonates,<sup>13,14</sup> but is limited by the fact that the phosphonic acid must melt rather than decompose at elevated temperatures; most amino-phosphonic acids decompose rather than melt and, hence, are not suited to this method.

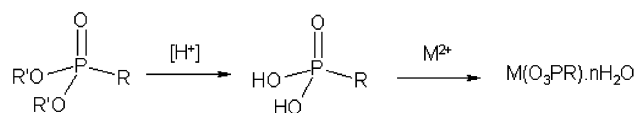
The majority of the M(II) phosphonates reported up to 1995 were lamellar in nature with the phosphonate anion pendant in the interlayer region. The structure of these materials is very similar to that observed in the M(IV) phosphonates, with an octahedral metal atom co-ordinated with oxygen, but differ in that some of the phosphonate oxygen atoms are shared between two metal atoms and that the co-ordination sphere of the metal contains a reversibly removable water molecule.<sup>11,15</sup>

In 1994, Bujoli *et al.* reported the first zeolite-like microporous phosphonate,  $\beta$ -Cu(O<sub>3</sub>PCH<sub>3</sub>).<sup>16</sup> In the same year, Maeda *et al.* reported the synthesis of  $\beta$ -Al<sub>2</sub>(O<sub>3</sub>PCH<sub>3</sub>)<sub>2</sub> (known as AlMePO- $\beta$ ).<sup>17</sup> Both of these materials contain a hexagonal array of one dimensional channels with diameters of 5.97 and 6.5 Å, respectively. The following year, Zn(O<sub>3</sub>PC<sub>2</sub>H<sub>4</sub>NH<sub>2</sub>)·H<sub>2</sub>O<sup>18</sup> and AlMePO- $\alpha$ <sup>19</sup> were reported, with similar channel structures. These materials sparked an interest in the synthesis of porous metal phosphonates, and have led to the production of materials containing Cu,<sup>20,21</sup> Co,<sup>22,23</sup> Zn,<sup>24–26</sup> Pb,<sup>27</sup> Sn,<sup>28</sup> Mn,<sup>29,30</sup> Al<sup>31</sup> and U.<sup>32</sup>

Many of these materials have two main features in common. Firstly, they usually contain metal atoms in non-octahedral co-ordination environments; this is by no means a rule, as both AlMePO materials contain octahedrally and tetrahedrally co-ordinated Al atoms, and Zn(O<sub>3</sub>PCH<sub>2</sub>OH) contains only octahedrally co-ordinated Zn atoms. Secondly, the organic phosphonate chains contain functional groups that act as Lewis bases and co-ordinate to the metal ions in addition to the PO<sub>3</sub> groups. This can lead to cross-linking and results in the formation of porous materials. Many of the porous materials reported to date include either carboxylic acid or carboxylate functional groups<sup>21–23,25–30</sup> (known as phosphonocarboxylates), which are ideally suited to this purpose.

It is our opinion that these properties of the metals and the phosphonate anions (or a combination of the two) can be exploited as a coherent strategy towards the synthesis of new porous materials.

Unlike tetravalent metal phosphonates, attempts at producing divalent metal-containing porous materials using diphosphonic acids have met with more success [*e.g.* Co<sub>2</sub>(O<sub>3</sub>PCH<sub>2</sub>PO<sub>3</sub>)·H<sub>2</sub>O<sup>33</sup> and Zn(O<sub>3</sub>PC<sub>6</sub>H<sub>4</sub>PO<sub>3</sub>)·2H<sub>2</sub>O<sup>34</sup>]. These are essentially pillared lamellar materials with a regular pore structure, although the



**Scheme 1** *In situ* hydrolysis of dialkylphosphonate esters and subsequent reaction with M<sup>2+</sup> to form metal phosphonates.

pores tend to be fairly small due to the size of the organic group or the close packing of the pillars in the organic layer.

In this paper, we describe the synthesis and characterisation of some new metal phosphonates that were made employing a strategy that uses bi-functional phosphonic acids and metals that can adopt non-octahedral co-ordination. The materials have been prepared by hydrothermal methods, in some cases using dialkylphosphonates as starting material. During the course of the hydrothermal treatment, the acidity of the metal solution helps effect the hydrolysis of the phosphonate to produce the phosphonic acid *in situ* (Scheme 1). This approach was derived from a method used to synthesise Zr phosphonates directly from dialkylphosphonates in which a mineral acid was added to a mixture of zirconium oxychloride and a dialkylphosphonate to carry out the hydrolysis.<sup>35</sup> In several cases, the synthetic methods used have enabled the synthesis of iso-structural phosphonates containing different metals. Investigations have also been carried out into the possibility of doping heterometals (such as cobalt) into phosphonates with known structures.

## Experimental

### Synthesis of metal phosphonates by hydrothermal decomposition of dialkylphosphonates

In a typical experiment, 3.7 mmol of a divalent metal acetate [Zn(CH<sub>3</sub>CO<sub>2</sub>)<sub>2</sub>·2H<sub>2</sub>O, Co(CH<sub>3</sub>CO<sub>2</sub>)<sub>2</sub>·4H<sub>2</sub>O, Cu(CH<sub>3</sub>CO<sub>2</sub>)<sub>2</sub>·H<sub>2</sub>O or Mn(CH<sub>3</sub>CO<sub>2</sub>)<sub>2</sub>] is dissolved in 10 ml distilled water. To this solution, 3.7 mmol of the dialkylphosphonate ester is added. The resulting mixture is placed in a Teflon-lined stainless steel autoclave, which has a capacity of 23 ml. The reaction mixture is heated under autogeneous pressure at 433 K for a period of 48 hours, after which it is removed and allowed to cool. The product is recovered by filtration and washed with water.

### Variations of the synthetic method used for materials containing a mixture of M<sup>II</sup> cations

In a typical preparation, acetates of the required metals are added to 10 ml distilled water such that the combined quantity of M<sup>II</sup> cations is 3.7 mmol. An equivalent quantity of the desired phosphonate is added and the solution treated in the manner described previously. After the heating process is complete, the autoclave is removed from the oven and the products recovered in the manner described above. It is noticeable that the products are not a single phase, especially where diethyl cyanomethylphosphonate is used in the synthesis. The products contain a blue phase and a polycrystalline pink phase; the quantity of pink material increases with the quantity of Co used in the preparation. The products from Co doping of Zn(O<sub>3</sub>PCH<sub>2</sub>OH) are also mixed, though it is not so readily apparent since both products are pink in colour. The pink impurity materials have not been characterised, but are assumed to be phosphonates that contain predominantly Co, with little or no Zn.

### Synthesis of Zn<sub>3</sub>(O<sub>3</sub>PCH<sub>2</sub>CO<sub>2</sub>)<sub>2</sub>·nH<sub>2</sub>O (n = 3, 4)

0.518 g of phosphonoacetic acid was added to a solution of 0.81 g zinc acetate in 10 ml distilled water. The resulting solution was placed in a Teflon-lined stainless steel autoclave, which has a capacity of 23 ml. The reaction mixture was heated

under autogenous pressure at 433 K for a period of 48 h, after which it was removed and allowed to cool. The product was recovered by filtration and washed with water.

### Sample characterisation

Infrared spectra of all samples were recorded using a Nicolet 5DXC spectrometer. Samples were mounted as self-supporting KBr disks which contained *ca.* 1% sample by mass.

The metal content of the samples was determined by atomic absorption spectroscopy and ICP spectroscopy. CHN contents were determined using a Carlo Erba 1011 analyser.

### Single crystal X-ray diffraction studies

All samples were examined under a microscope and in the case of Cu(O<sub>3</sub>PCH<sub>2</sub>OH), this inspection revealed the presence of only very small (dimensions in the region of 10 μm) single crystals. These crystals were investigated using microcrystal diffraction facilities at Daresbury SRS.<sup>36</sup> A laboratory instrument was employed for the larger crystals [Zn(O<sub>3</sub>PCH<sub>2</sub>C(O)NH<sub>2</sub>)·H<sub>2</sub>O and Zn<sub>3</sub>(O<sub>3</sub>PCH<sub>2</sub>CO<sub>2</sub>)<sub>2</sub>·nH<sub>2</sub>O].

**Synchrotron microcrystal diffraction data acquisition.** Data were collected at low temperature (150 K) using a Bruker AXS SMART CCD area-detector diffractometer on the high-flux single crystal diffraction station 9.8 at the CLRC Daresbury Laboratory Synchrotron Radiation Source, Cheshire, UK. The experiments used X-rays of wavelength 0.68770 Å selected by a horizontally focusing silicon (111) monochromator and vertically focused by a cylindrically bent palladium-coated zerodur mirror. The data set covered a hemisphere of reciprocal space with several series of exposures. Corrections were made for the synchrotron beam intensity decay as part of the standard inter-frame scaling procedures.

**Laboratory data acquisition.** Measurements were carried out at 298 K on a Rigaku R-Axis II image plate diffractometer using a rotating anode generator with Mo-Kα radiation (λ = 0.71069 Å). The crystals were mounted on a glass fibre using an epoxy resin, and 36 images recorded covering 180° of crystal rotation.

**Structure solution.** Structure solution was carried out by direct methods using the SHELXS program,<sup>37</sup> (employed within the WINGX suite of programs<sup>38</sup>) and revealed the location of all non-hydrogen atoms, which were refined anisotropically. The H atoms were typically either located in the Fourier difference map or placed geometrically. Subsequent refinement of the displacement parameters of the hydrogen atoms was carried out isotropically in all cases. Some hydrogen atoms which could not be located in the Fourier difference map are omitted due to disorder.

CCDC reference numbers 184731–184733.

See <http://www.rsc.org/suppdata/jm/b2/b204131f/> for crystallographic data in CIF or other electronic format.

### Powder X-ray diffraction studies

M(O<sub>3</sub>PCH<sub>2</sub>OH) (M = Mn, Co) could not be prepared as crystals of sufficient quality for single crystal analysis, hence, structural characterisation was carried out using powder X-ray diffraction data.

**Data acquisition.** The data for the Mn-containing sample were collected on a Bruker AXS D5000 diffractometer at 298 K using Ge-monochromated Cu-Kα<sub>1</sub> radiation (λ = 1.54056 Å) operating in transmission mode with a linear position-sensitive detector covering 8° in 2θ. The sample was mounted in a flat disc between two pieces of tape, and data collected over the range 4 < 2θ < 54° in steps of 0.01947°.

The data for the Co-containing sample were collected with a Stoe diffractometer at 298 K using Ge-monochromated Fe-Kα<sub>1</sub> radiation (λ = 1.936 Å) operating in transmission mode with a linear position sensitive detector covering 6° in 2θ. The sample was mounted in a 0.5 mm glass capillary, and data collected over the range 5 < 2θ < 110° in steps of 0.02°.

**Rietveld refinement.** Inspection of these powder X-ray diffraction patterns shows that both the Mn and Co materials are isostructural to Zn(O<sub>3</sub>PCH<sub>2</sub>OH).<sup>24</sup> Hence, Rietveld refinement of both data sets was carried out using the GSAS program package,<sup>39</sup> with the structure of Zn(O<sub>3</sub>PCH<sub>2</sub>OH) used as an initial starting model for refinement. All atom positions were refined using geometric restraints (on interatomic bond lengths and geminal bond angles in the hydroxymethylphosphonate group) and isotropic displacement parameters (refined for non-H only) constrained by atom type. For the Co material, an absorption coefficient was also refined. The final refined agreement factors and crystallographic information derived from these analyses is given in Table 1, and the final Rietveld profile fits shown in Fig. 2. This analysis clearly shows that the Co and Mn derivatives have the same structure as Zn(O<sub>3</sub>PCH<sub>2</sub>OH).<sup>24</sup>

## Results

### Structure of M(O<sub>3</sub>PCH<sub>2</sub>OH) [M = Cu, Zn, Mn, Co]

The Cu, Mn and Co materials are isostructural to that reported elsewhere for Zn(O<sub>3</sub>PCH<sub>2</sub>OH).<sup>24</sup> All four M(O<sub>3</sub>PCH<sub>2</sub>OH) structures crystallise in the trigonal space group *R* $\bar{3}$  (no. 148), with lattice parameters shown in Table 1. The metal atoms are in a distorted octahedral co-ordination environment, and adjacent metal atoms are connected by one O–P–O bridge and two bridging oxygen atoms from the phosphonate groups. The

**Table 1** Crystallographic data for M(O<sub>3</sub>PCH<sub>2</sub>OH) [M = Zn,<sup>24</sup> Cu, Co, Mn]

Empirical formula	CH <sub>3</sub> O <sub>4</sub> PZn	CH <sub>3</sub> O <sub>4</sub> PCu	CH <sub>3</sub> O <sub>4</sub> PCo <sup>a</sup>	CH <sub>3</sub> O <sub>4</sub> PMn <sup>a</sup>
Fw	175.40	173.54	170.04	166.04
Space group	<i>R</i> $\bar{3}$ (no.148)	<i>R</i> $\bar{3}$ (no.148)	<i>R</i> $\bar{3}$ (no.148)	<i>R</i> $\bar{3}$ (no.148)
<i>a</i> /Å	15.970(2)	16.1240(17)	16.0312(1)	16.3462(9)
<i>c</i> /Å	7.783(2)	7.6023(11)	7.7499(1)	8.0174(4)
<i>V</i> /Å <sup>3</sup>	1719.1(4)	1711.7(4)	1724.88(5)	1855.2(3)
<i>Z</i>	18	18	18	18
Temp./K	298(2)	150 (2)	298	298
λ/Å	0.71069	0.68770, synchrotron	1.936	1.54056
ρ <sub>calcd</sub> /g cm <sup>-3</sup>	3.05	3.03	2.947	2.675
μ/cm <sup>-1</sup>	6.715	6.028	—	—
Meas. refl / unique refl.	3567 / 678	3951 / 883	244 / —	93 / —
<i>R</i> <sub>int</sub>	0.0234	0.0354	0.0901 ( <i>R</i> <sub>F2</sub> )	0.1594 ( <i>R</i> <sub>F2</sub> )
<i>R</i> ( <i>F</i> <sub>o</sub> ) <sub>all</sub>	0.020	0.0339	0.0702 ( <i>R</i> <sub>p</sub> )	0.0230 ( <i>R</i> <sub>p</sub> )
w <i>R</i> ( <i>F</i> <sub>o</sub> <sup>2</sup> ) <sub>all</sub>	0.051	0.0782	0.0928 ( <i>R</i> <sub>wp</sub> )	0.0293 ( <i>R</i> <sub>wp</sub> )

<sup>a</sup>Data from Rietveld refinement of powder XRD data against structural model obtained for Zn(O<sub>3</sub>PCH<sub>2</sub>OH).

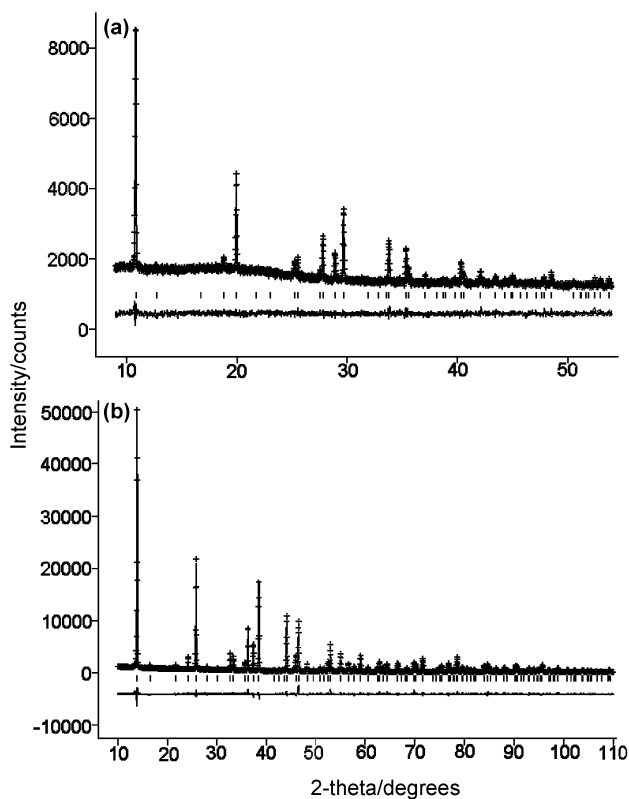


**Fig. 2** Final observed (crosses), calculated (solid line) and difference (below) X-ray powder diffraction profiles for the final Rietveld refinements of  $M(O_3PCH_2OH)$  [ $M = Mn$  (a),  $Co$  (b)]. Reflection positions are also marked.

oxygen atoms of the phosphonate group have (122) connectivity,<sup>40</sup> *i.e.* two of them are shared between two metal atoms. Two of the phosphonate groups act as bridges between infinite zigzag chains of  $M$  atoms, which are approximately 3.2 Å apart, in the [001] direction. Within these chains, adjacent  $M$  atoms are connected by one O–P–O and two O bridges. The chains are then cross-linked by O–P–O and P–C–O–M bridges, forming hexagonal channels parallel to the  $c$  axis, which have a diameter of *ca.* 5.7 Å between two opposite methylene C atoms (Fig. 3).

Five of the six co-ordination sites around the metal are thus occupied by phosphonate oxygens and the sixth is occupied by the oxygen of the hydroxyl group of the phosphonate anion (the C–O bond can be seen in Fig. 3). Hence, the functional group is bound to the inorganic part of the framework rather

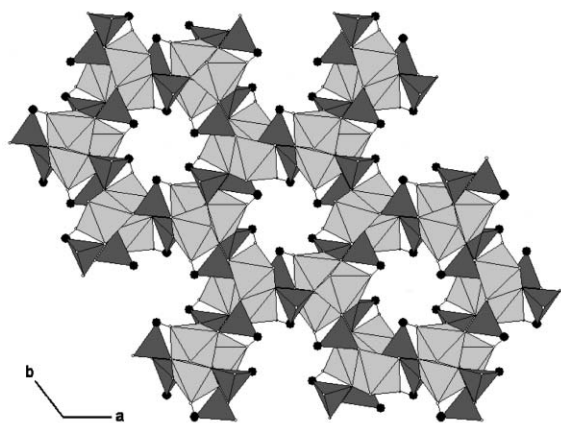


**Fig. 3** Polyhedral view of the structure of  $M(O_3PCH_2OH)$  [ $M = Cu, Zn, Co, Mn$ ], showing the channel structure. Light grey polyhedra are  $MO_6$  and dark grey polyhedra are  $O_3PC$  tetrahedra. Black circles are C atoms. Hydrogen atoms are omitted for clarity.

**Table 2** Crystallographic data for  $Zn(O_3PCH_2C(O)NH_2) \cdot H_2O$

Empirical formula	$C_2H_6NO_5PZn$
Fw	220.42
Space group	$Pna2_1$ (no. 33)
$a/\text{Å}$	9.5560(13)
$b/\text{Å}$	12.600(2)
$c/\text{Å}$	5.2318(8)
$V/\text{Å}^3$	630.46(17)
$Z$	4
Temp./K	298(2)
$\lambda/\text{Å}$	0.71069
$\rho_{\text{calcd}}/\text{g cm}^{-3}$	2.322
$\mu/\text{cm}^{-1}$	4.111
Meas. refl. / unique refl.	3659 / 1109
$R_{\text{int}}$	0.0517
$R(F_o)_{\text{all}}$	0.0313
$wR(F_o^2)_{\text{all}}$	0.0833

than being directed into the channels as observed in  $\beta\text{-Cu}(O_3PCH_3)$ .<sup>16</sup> The hydrogen atom of the –OH group could not be located in the Fourier difference map.

### Structure of $Zn(O_3PCH_2C(O)NH_2) \cdot H_2O$

The synthesis of this material was carried out using diethyl cyanomethylphosphonate, with the intention of preparing a material containing nitrile functional groups. The single crystal analysis carried out on the product showed that the phosphonate had been hydrolysed under the conditions of the reaction to form an amide. This is confirmed by the CHN analysis of the product (calculated: C 10.90, H 2.74, N 6.36; observed; C 11.00, H 2.21, N 5.96%) and IR spectroscopy (*vide infra*).

This material crystallises in the orthorhombic spacegroup  $Pna2_1$  (no. 33), with cell parameters as shown in Table 2. The metal atoms have tetrahedral co-ordination environments, with Zn–O bond lengths in the range 1.955(3)–1.959(4) Å; the phosphonate connectivity is (111).

Three of the four co-ordination sites are occupied by  $\text{PO}_3$  oxygen atoms from three different phosphonate anions, which leads to the formation of chains aligned in the  $c$  direction. The fourth co-ordination site is occupied by either a nitrogen atom or the carboxyl oxygen (as discussed below). The occupation of the fourth site by the oxygen or nitrogen of the amide group leads to a cross-linking of the chains and the formation of two orthogonal channel systems; one parallel to the  $a$  axis (Fig. 4) and the other parallel to the  $c$  axis (Fig 5). The smaller channels, running in the [100] direction, have a diameter of *ca.* 3.5 Å and are roughly triangular in shape, with one ‘corner’ being occupied by the –NH<sub>2</sub> or C=O moieties of the amide groups. The second channel type, running in the [001] direction, has an elongated ‘dumbbell’ shape, with dimensions of *ca.* 13.5 × 3.9 Å (the H··H distance is *ca.* 2.9 Å). Water molecules are located at the intersections of the two channel systems.

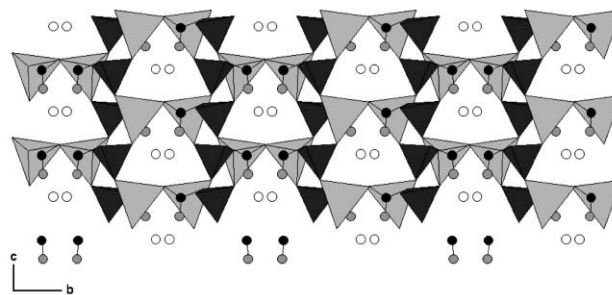


**Fig. 4** Polyhedral view of the structure of  $Zn(O_3PCH_2C(O)NH_2) \cdot H_2O$ , showing the channel structure in the [100] direction. Light grey polyhedra are  $ZnO_4$  and dark grey polyhedra are  $O_3PC$  tetrahedra. Black circles are C, grey circles are N and white circles are O. Hydrogen atoms are omitted for clarity.

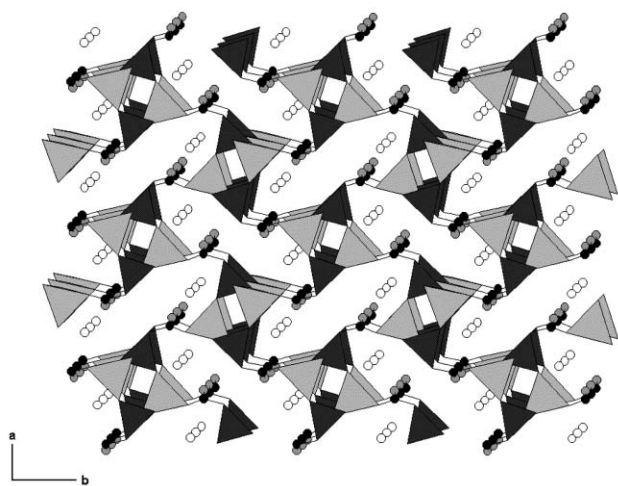


**Fig. 5** Polyhedral view of the structure of  $\text{Zn}(\text{O}_3\text{PCH}_2\text{C}(\text{O})\text{NH}_2) \cdot \text{H}_2\text{O}$ , showing the channel structure in the [001] direction. Light grey polyhedra are  $\text{ZnO}_4$  and dark grey polyhedra are  $\text{O}_3\text{PC}$  tetrahedra. Black circles are C, grey circles are N and white circles are O. Hydrogen atoms are omitted for clarity.

In this structure, the amide C–O and C–N bonds are approximately equal in length [1.267(8) and 1.253(11) Å], although single C–O and C–N bonds should be longer than the corresponding C=NH or C=O bonds. Structure refinement could not conclusively discriminate between the O and N atoms. Possible reasons include: (i) static disorder, with co-ordination to Zn by O and N being equally likely, (ii) flipping about the C–C bond, resulting in dynamic disorder between the O and N atoms, (iii) tautomerism of the amide group, with the average bond length observed lying between a single and a double bond or (iv) a combination of the above reasons.

The IR spectrum (Fig. 6) contains peaks due to C–H(str) at 2996, 2952 and 2844  $\text{cm}^{-1}$ , P–C(str) at 1436  $\text{cm}^{-1}$  and P–O(str) as a series of sharp bands in the region 1150–950  $\text{cm}^{-1}$ .<sup>41</sup> There is no trace in the spectrum of a peak at 2256  $\text{cm}^{-1}$ , which is observed in the spectrum of diethyl cyanomethylphosphonate and arises from the  $\text{C}\equiv\text{N}$  stretching mode. The main feature is the peak at 1598  $\text{cm}^{-1}$  arising from the stretching mode of the carbonyl group. The C=O stretching frequency is lower than one might expect to observe for an amide, but this effect has been previously observed in the IR spectra of the carboxylic acid-containing materials  $\text{Zn}(\text{O}_3\text{P}(\text{CH}_2)_2\text{CO}_2\text{H}) \cdot 1.5\text{H}_2\text{O}$ <sup>25</sup> and  $\text{Al}(\text{O}_3\text{PCH}_2\text{CO}_2) \cdot 3\text{H}_2\text{O}$ .<sup>42</sup> This reduction in frequency arises from the co-ordination of the carbonyl group to a metal atom in a neighbouring phosphonate chain, as seen in the structural analysis, and is also reflected in the C=O bond length, which is slightly longer than one would expect for a free amide. This evidence suggests that in  $\text{Zn}(\text{O}_3\text{PCH}_2\text{C}(\text{O})\text{NH}_2) \cdot \text{H}_2\text{O}$ , it is the

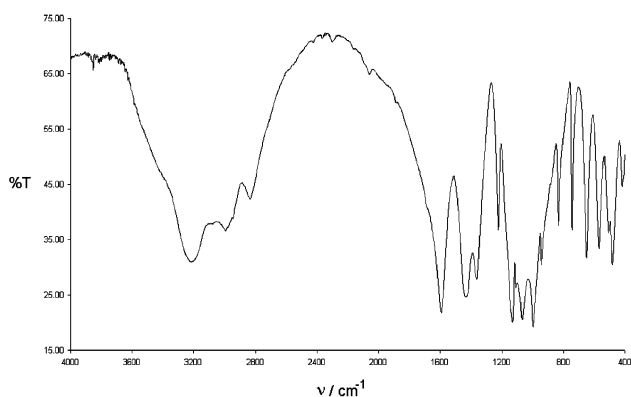


**Fig. 6** FT-IR spectrum for  $\text{Zn}(\text{O}_3\text{PCH}_2\text{C}(\text{O})\text{NH}_2) \cdot \text{H}_2\text{O}$ .

carbonyl oxygen that bonds to the Zn atoms rather than the N atom.

Further information regarding the bonding around the Zn atom can be obtained from  $^{15}\text{N}$  MAS NMR spectroscopy. Only one peak was present in the  $^{15}\text{N}$  solid state NMR spectrum ( $\delta = -355.7$  ppm), lying between the ranges expected for amides and imines, and implying that only one nitrogen environment is present.

The most consistent explanation for these spectroscopic results and the similarity of the C–O and C–N bonds is probably tautomerism. Hydrogen atoms could not be located for the amide group and it is hoped that neutron diffraction experiments will shed light on their positions and, hence, the real picture regarding the co-ordination. Rietveld refinement of this structure has confirmed that the sample is a single phase.

Attempts to synthesise other analogues containing other metals have met with limited success. A nickel-based material has been synthesised, but only as the minor component in a two-phase mixture.<sup>43</sup> An attempt to produce a Co analogue of this material resulted in the formation of a pink product, rather than the blue one that would be expected from a knowledge of the structure. The colour of the material is consistent with the octahedral co-ordination environment of metal atoms in lamellar  $\text{M}^{\text{II}}$  phosphonates. The structure of this phase is unknown, but powder X-ray diffraction suggests that the material is layered in nature.

The hydrogen atoms associated with the nitrogen of the amide group were not located in the Fourier difference map and were not placed geometrically due to disorder in the N/O positions.

#### Structure of $\text{Zn}_3(\text{O}_3\text{PCH}_2\text{CO}_2)_2 \cdot n\text{H}_2\text{O}$ ( $n = 3, 4$ )

This material crystallises in the space group  $P2_1/n$  (no. 14) with the lattice parameters listed in Table 3. The Zn atoms in this material are present in more than one co-ordination environment. The asymmetric unit contains three crystallographically distinct Zn atoms [one tetrahedral, one octahedral and a third (see below) which is either 5- or 6-co-ordinate depending upon the level of hydration of the material] and two distinct phosphonate anions [one with (111) connectivity and the other with (122)].

The structure is constructed from complex sub-units that contain six Zn atoms (two of each crystallographically distinct type). The core of the sub-unit is composed of two edge sharing octahedrally co-ordinated metal atoms [ $\text{Zn}(2)$ ]. These two distorted octahedra [ $\text{Zn}-\text{O}$  distances = 2.085(5)–2.134(5) Å] are further connected by phosphonate groups. The axial site of one Zn(2) is occupied by a phosphate oxygen and is linked to one of the axial sites of the other Zn(2) via a Zn–O–P–C–O–Zn bridge. A similar arrangement is observed for the other axial sites in the opposite direction (shown schematically in Fig. 7). Another link between the octahedra is observed in the form of

**Table 3** Crystallographic data for  $\text{Zn}_3(\text{O}_3\text{PCH}_2\text{CO}_2)_2 \cdot n\text{H}_2\text{O}$

Empirical formula	$\text{C}_4\text{H}_{6.76}\text{O}_{11.38}\text{P}_2\text{Zn}_3$
Fw	495.03
Space group	$P2_1/n$ (no. 14)
$a/\text{Å}$	4.9250(3)
$b/\text{Å}$	22.0972(3)
$c/\text{Å}$	12.9038(3)
$\beta/^\circ$	99.245(2)
$V/\text{Å}^3$	1386.06(9)
Z	8
Temp./K	293(2)
$\lambda/\text{Å}$	0.71069
$\rho_{\text{calcd}}/\text{g cm}^{-3}$	2.372
$\mu/\text{cm}^{-1}$	5.431
Meas. refl / unique refl.	7952 / 3399
$R_{\text{int}}$	0.0487
$R(F_o)_{\text{all}}$	0.0778
$wR(F_o^2)_{\text{all}}$	0.1589

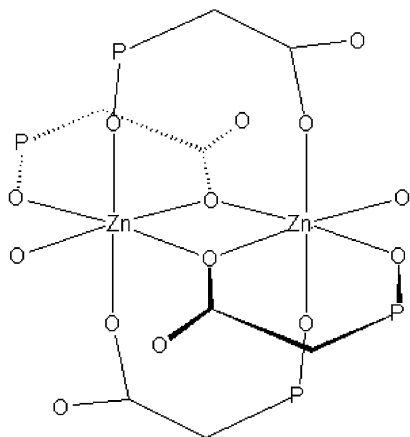


**Fig. 7** Schematic representation of the bonding between the two central  $\text{ZnO}_6$  octahedra in  $\text{Zn}_3(\text{O}_3\text{PCH}_2\text{CO}_2)_2 \cdot n\text{H}_2\text{O}$ .

two phosphonate molecules co-ordinating in a bidentate manner. The O atoms that are common to both polyhedra, due to edge sharing, are from  $\text{PO}_3$  groups. The remainder of the phosphonate moiety loops round and one of the carboxyl oxygen atoms is co-ordinated to an adjacent equatorial site. These O–P–C–O bridges are oriented approximately  $90^\circ$  to the bridges linking the axial sites (Fig 7).

Each Zn(1) polyhedron [ $\text{Zn–O} = 1.968(5)–2.199(3) \text{ \AA}$ ] is connected to the core by edge sharing with one of the Zn(2) $\text{O}_6$  octahedra and the Zn(3)-centred  $\text{ZnO}_4$  tetrahedra [ $\text{Zn–O} = 1.927(5)–2.016(5) \text{ \AA}$ ] are linked to the core by corner sharing. They are also additionally bound to the core by a phosphonate anion (Fig 8).

The sub-units form columns by stacking in the [100] direction. The units are linked by  $\text{PO}_3$  groups and, whilst they are approximately planar, they are oriented at an angle with respect to the (100) plane (Fig. 9). The columns are then crosslinked to other columns *via* the Zn(3) atoms being co-ordinated by a carboxylate anion from an adjacent column (Fig. 9). The resulting channels, aligned in the [100] direction have and rhombohedral shape with dimensions of *ca.*  $10.0 \text{ \AA} \times 6.8 \text{ \AA}$  (Fig. 8).

Zn(1) co-ordination is disordered with either 5 or 6 oxygen atoms being involved. The 5-co-ordinate component is in the form of a distorted square bipyramid, whereas the 6-co-ordinate component is distorted octahedral. The disorder arises due to partial occupancy of three oxygen atoms (all water molecules) in the equatorial plane shared by the co-ordination polyhedra. The major component is 5-co-ordinate with 80% occupancy.

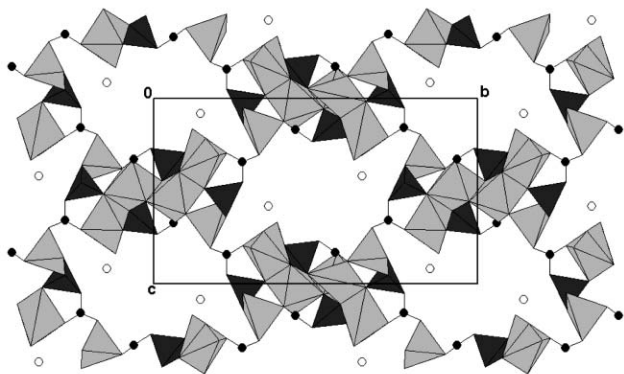


**Fig. 8** Polyhedral view of the structure of  $\text{Zn}_3(\text{O}_3\text{PCH}_2\text{CO}_2)_2 \cdot n\text{H}_2\text{O}$ , showing the channel structure in the [100] direction. Light grey polyhedra are  $\text{ZnO}_4$  and dark grey polyhedra are  $\text{O}_3\text{PC}$  tetrahedra. Black circles are C and white circles are O. Hydrogen atoms are omitted for clarity.

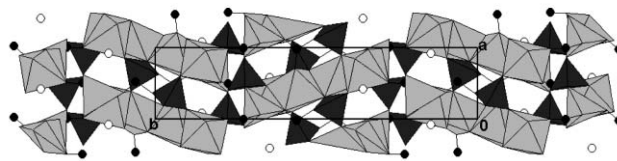


**Fig. 9** Polyhedral view of the structure of  $\text{Zn}_3(\text{O}_3\text{PCH}_2\text{CO}_2)_2 \cdot n\text{H}_2\text{O}$  showing the channel structure in the [001] direction. Light grey polyhedra are  $\text{ZnO}_4$  and dark grey polyhedra are  $\text{O}_3\text{PC}$  tetrahedra. Black circles are C and white circles are O. Hydrogen atoms are omitted for clarity.

The final refinement contains a number of large residual peaks ( $1.8–2.4 \text{ e \AA}^{-3}$ ) which are located at distances of  $1 \text{ \AA}$  or less from the Zn atoms.

### Inclusion of Co in frameworks of Zn phosphonates

The colour of products resulting from inclusion of Co in the reaction mixture depends on the co-ordination environment of the Co in the resulting material. Co included in  $\text{Zn}(\text{O}_3\text{PCH}_2\text{OH})$  results in the formation of pink crystals; in  $\text{Zn}(\text{O}_3\text{PCH}_2\text{C}(\text{O})\text{NH}_2) \cdot \text{H}_2\text{O}$ , the crystals are blue, and in  $\text{Zn}_3(\text{O}_3\text{PCH}_2\text{COO}) \cdot n\text{H}_2\text{O}$ , they are purple in colour. The colours are indicative of wholly octahedral, wholly tetrahedral and a mixture of 5- and 6-co-ordinate environments, respectively. The colours of the samples become darker as the Co content is increased, though visual inspection reveals some variation in the intensity for different crystals from the same sample. Single crystal analysis of Co-doped  $\text{Zn}(\text{O}_3\text{PCH}_2\text{OH})$  and  $\text{Zn}(\text{O}_3\text{PCH}_2\text{C}(\text{O})\text{NH}_2) \cdot \text{H}_2\text{O}$  confirms that Co replaces some Zn in framework sites and is not present in extra-framework sites.

In both these cases, it is also apparent that there is a second phase present in the products. It is polycrystalline, pink and can be difficult to observe in the case of Co-doped  $\text{Zn}(\text{O}_3\text{PCH}_2\text{OH})$ , since both phases are pink in colour. The quantity of the impurity phases increases with the quantity of Co included in the synthesis mixture. The pink material in Co-doped  $\text{Zn}(\text{O}_3\text{PCH}_2\text{C}(\text{O})\text{NH}_2) \cdot \text{H}_2\text{O}$  can be preferentially removed by suspension of the sample in 10 ml of 0.5 M acetic acid and placing it in an ultrasound bath for 5 min. AAS analysis of the remaining blue Co-doped  $\text{Zn}(\text{O}_3\text{PCH}_2\text{C}(\text{O})\text{NH}_2) \cdot \text{H}_2\text{O}$  phase shows that approximately half of the Co included in the synthesis mixture is taken up in the products (Table 4). Single crystal analysis of one of the blue crystals confirmed that the structure was identical to that of the parent material, with Co isomorphously located in the tetrahedral Zn sites.

### Discussion

$\text{M}(\text{O}_3\text{PCH}_2\text{OH})$  materials can be synthesised with a number of metals; here we have reported Co, Mn and Cu, and shown them to be isostructural to the Zn-based material we reported elsewhere.<sup>24</sup> Work is being undertaken to characterise other divalent metal systems, such as Fe and Ni, and to investigate whether the oxidation state of various metals can be changed *in situ*. These materials also display octahedral co-ordination of the metal atoms; a feature rarely seen in porous phosphonates.

**Table 4** Co contents of the synthesis mixtures and crystalline products for  $\text{Zn}_{1-x}\text{Co}_x(\text{O}_3\text{PCH}_2\text{C}(\text{O})\text{NH}_2) \cdot \text{H}_2\text{O}$

Mol% Co in reaction mixture	Mol% Co in products <sup>a</sup>	Formula
1	0.4	$\text{Zn}_{0.996}\text{Co}_{0.004}(\text{O}_3\text{PCH}_2\text{CONH}_2) \cdot \text{H}_2\text{O}$
2	0.7	$\text{Zn}_{0.993}\text{Co}_{0.007}(\text{O}_3\text{PCH}_2\text{CONH}_2) \cdot \text{H}_2\text{O}$
3	1.8	$\text{Zn}_{0.982}\text{Co}_{0.018}(\text{O}_3\text{PCH}_2\text{CONH}_2) \cdot \text{H}_2\text{O}$
5	2.3	$\text{Zn}_{0.977}\text{Co}_{0.023}(\text{O}_3\text{PCH}_2\text{CONH}_2) \cdot \text{H}_2\text{O}$
20	8.4	$\text{Zn}_{0.917}\text{Co}_{0.083}(\text{O}_3\text{PCH}_2\text{CONH}_2) \cdot \text{H}_2\text{O}$
50	27.1	$\text{Zn}_{0.729}\text{Co}_{0.271}(\text{O}_3\text{PCH}_2\text{CONH}_2) \cdot \text{H}_2\text{O}$

<sup>a</sup>  $\pm 0.1\%$ .

To date,  $M(O_3PCH_2C(O)NH_2) \cdot H_2O$  has only been synthesised with  $M = Zn$  or  $Ni$ ; attempts at synthesis with other metals have been unsuccessful. The difficult preparation of this material is highlighted by the fact that the  $Ni$  derivative can only be prepared as a minor component of a mixture of products.<sup>43</sup> The structure is complicated by the similarity in the length of the  $C-N$  and  $C-O$  bonds, which makes the exact nature of the bonding around the  $Zn$  atoms difficult to determine.

The structure of  $Zn_3(O_3PCH_2CO_2)_2 \cdot nH_2O$  is not observed for other phosphonocarboxylates.  $Zn_3(O_3PCH_2CO_2)_2 \cdot nH_2O$  has features in common with other materials containing different metals but with similar stoichiometries, e.g.  $Mn_3(O_3PCH_2CO_2)_2$ <sup>29,30</sup> and  $Pb_3(O_3PCH_2CO_2)_2$ .<sup>27</sup> They all contain metal atoms in three co-ordination environments, and  $Mn_3(O_3PCH_2CO_2)_2$  contains two edge-sharing  $MnO_6$  octahedra. However, there are also significant differences, the most obvious of which is that the  $Zn$ -based material is hydrated, with the co-ordination environment of one of the  $Zn$  atoms dependent on the level of hydration. The basic structure of  $Mn_3(O_3PCH_2CO_2)_2$  differs from that of  $Zn_3(O_3PCH_2CO_2)_2 \cdot nH_2O$  in that the  $Mn$ -based sample is made up from layers in the  $ac$  plane, crosslinked in the  $b$  direction, thereby forming narrow channels in the  $[100]$  direction. The dimensions of these channels are approximately  $10 \times 3.8 \text{ \AA}$ .<sup>30</sup> In the  $Zn$ -based materials, the channels in the  $[100]$  direction are somewhat larger and are formed by cross-linking of columns which are aligned in the same direction.

There appears to be a rich but largely untapped structural chemistry in the phosphonocarboxylates. A few of these materials have been shown to be porous, with different structures. Given the possible variations in the identity of the metal and the nature of the carboxylate (e.g. alkyl chain length, cyclic carbonates *etc.*), there are potentially a large number of structures waiting to be discovered.

The synthesis of metal phosphonates directly from dialkylphosphonate esters is a useful route that avoids the necessity of purifying phosphonic acids. The weak acidity of the metal solutions is sufficient to carry out the hydrolysis of the ester. The use of acetates in the hydrothermal preparation of phosphonate materials has also proven to be beneficial. The pH of the solutions after reaction is somewhat less acidic than for similar reactions in which chlorides or nitrates have been used. In several instances, we have discovered that the use of a metal acetate results in the formation of a solid product where a chloride (or nitrate) will not. It has been demonstrated previously that the nature of the products of hydrothermal syntheses can be affected by the nature of the starting material.<sup>9,10</sup> Divalent metal phosphonates are known to be susceptible to acid attack, hence the acidity of the final reaction solution effects the crystallisation of the products.

Samples of  $Zn_{1-x}Co_x(O_3PCH_2C(O)NH_2) \cdot H_2O$  synthesised in this work seem to be more resilient to dissolution by acid than the  $Co$  impurities, which are thought to be layered in structure. Neither the product nor the impurities arising from the doping of  $Zn(O_3PCH_2OH)$  are soluble in acetic acid. It has been shown that it is possible to synthesise  $Co(O_3PCH_2OH)$  and it is thought that this phase occurs as an impurity of a darker pink colour. The structural similarity of the two phases means that one cannot be preferentially removed by treatment with acid.

## Conclusions

The application of a strategy involving the use of multifunctional phosphonate anions in conjunction with cations that can adopt more than one type of co-ordination environment has led to the synthesis of two new porous materials (and three additional examples of a known structure containing different

metals). The hydrolysis of dialkylphosphonates during the course of the hydrothermal synthetic procedure removes the need to produce pure phosphonic acids before a metal phosphonate can be synthesised; this can often be difficult to achieve. So far, this method provides some consistency, allowing isostructural materials containing different metal cations to be synthesised.

The porous nature of all the materials reported in this paper makes use of the bifunctional nature of the phosphonate anion. In the case of  $M(O_3PCH_2OH)$  and  $Zn_3(O_3PCH_2CO_2)_2 \cdot nH_2O$ , the 'second' functional group is involved in co-ordination to metal atoms and any potential use of the group as a site for catalysis or further co-ordination is lost. In  $Zn_3(O_3PCH_2CO_2)_2 \cdot nH_2O$ , however, the removal of the water molecules surrounding the  $Zn(1)$  atoms could allow that site to be used for catalysis if it could be preferentially populated by a redox active metal.

There are several parameters involved in the solvothermal synthetic methods habitually employed in the synthesis of metal phosphonates, e.g. temperature, pH, metal salt, reactant ratios, solvent. Changing one or all of them can lead to new materials based on the same metals and phosphonate anions. Systematic investigations of these parameters, in conjunction with variations in the metal and organic functional group employed could lead to a large number of porous materials of widely varying chemical and structural properties.

One logical step forward is to use phosphonate anions that are trifunctional. The inherent danger is that all three groups might then become involved in co-ordination to metal atoms in the structure, with loss of the desired functionality. Successful use of trifunctional phosphonates with divalent metals has been demonstrated in the synthesis of  $Zn(O_3PCH_2CH(NH_3)COO)$  and  $Zn(O_3PC_2H_4CH(NH_3)COO)$ .<sup>26</sup> Work is currently being undertaken in this direction in our laboratory, and has recently proved successful. Further results will be published elsewhere.

## Acknowledgements

G. B. H. would like to thank the EPSRC for funding and the provision of a studentship for A. T. The authors would also like to thank the EPSRC single crystal diffraction service for data collection. M. J. T. would like to thank the Royal Society for the provision of a University Research Fellowship. The authors would also like to thank Dr A. D. Robertson (University of St. Andrews) and Dr S. Kitchin (University of Birmingham) for collecting  $Fe-K\alpha$  powder XRD and  $^{15}N$  MAS-NMR data, respectively.

## References

- 1 (a) S. Yamanaka, M. Matsunaga and M. Hattori, *J. Inorg. Nucl. Chem.*, 1976, **43**, 1343; (b) S. Yamanaka, M. Tsujimoto and M. Tanaka, *J. Inorg. Nucl. Chem.*, 1978, **41**, 605.
- 2 A. Clearfield and G. D. Smith, *Inorg. Chem.*, 1969, **8**, 431.
- 3 G. Alberti, U. Costantino, S. Alluli and N. Tomassini, *J. Inorg. Nucl. Chem.*, 1978, **40**, 1113.
- 4 M. B. Dines and P. DiGiacomo, *Polyhedron*, 1982, **1**, 62.
- 5 M. B. Dines and P. DiGiacomo, *Inorg. Chem.*, 1981, **20**, 92; M. B. Dines and P. C. Griffith, *Inorg. Chem.*, 1983, **22**, 567; M. B. Dines, R. E. Cooke and P. C. Griffith, *Inorg. Chem.*, 1983, **22**, 1003; M. B. Dines and P. C. Griffith, *Polyhedron*, 1983, **2**, 607.
- 6 A. Clearfield, *Chem. Mater.*, 1998, **10**, 2801.
- 7 G. B. Hix and K. D. M. Harris, unpublished results.
- 8 D. Cunningham, P. J. D. Hennelly and T. Deeney, *Inorg. Chim. Acta*, 1979, **37**, 95.
- 9 A. Cabeza, M. A. G. Aranda, S. Bruque, D. M. Poojary, A. Clearfield and J. Sanz, *Inorg. Chem.*, 1998, **37**, 4168.
- 10 N. Zakowsky, G. B. Hix and R. E. Morris, *J. Mater. Chem.*, 2000, **10**, 2375–2380.
- 11 G. B. Hix and K. D. M. Harris, *J. Mater. Chem.*, 1998, **8**, 579.
- 12 H. Hayashi and M. J. Hudson, *J. Mater. Chem.*, 1995, **5**, 115.
- 13 G. B. Hix, V. J. Carter, D. S. Wragg, R. E. Morris and P. A. Wright, *J. Mater. Chem.*, 1999, **9**, 179.

- 14 G. B. Hix, D. S. Wragg, I. Bull, R. E. Morris and P. A. Wright, *Chem. Commun.*, 1999, 2421.
- 15 G. Cao, H. Lee, V. M. Lynch and T. E. Mallouk, *Inorg. Chem.*, 1988, **27**, 2781.
- 16 J. Le Bideau, C. Payen, P. Palvadeau and B. Bujoli, *Inorg. Chem.*, 1994, **33**, 4885.
- 17 (a) K. Maeda, J. Akimoto, Y. Kiyozumi and F. Mizukami, *Angew. Chem., Int. Ed. Engl.*, 1994, **33**, 2335; (b) K. Maeda, J. Akimoto, Y. Kiyozumi and F. Mizukami, *Chem. Commun.*, 1995, 1033.
- 18 S. Drumel, P. Janvier, D. Deniaud and B. Bujoli, *Chem. Commun.*, 1995, 1051.
- 19 K. Maeda, J. Akimoto, Y. Kiyozumi and F. Mizukami, *Angew. Chem., Int. Ed. Engl.*, 1995, **34**, 1199.
- 20 P. Yin, L.-M. Zheng, S. Gao and X.-Q. Xin, *Chem. Commun.*, 2001, 2346.
- 21 M. Riou-Cavallec, M. Sanselme, N. Guillou and G. Férey, *Inorg. Chem.*, **40**, 723.
- 22 P. Rabu, P. Janvier and B. Bujoli, *J. Mater. Chem.*, 1999, **9**, 1323.
- 23 A. Distler and S. Sevov, *Chem. Commun.*, 1998, 959.
- 24 G. B. Hix, B. M. Kariuki, S. Kitchin and M. Tremayne, *Inorg. Chem.*, 2001, **40**, 1477.
- 25 S. Drumel, P. Janvier, P. Barboux, M. Bujoli-Doeuff and B. Bujoli, *Inorg. Chem.*, 1995, **34**, 148.
- 26 S. J. Hartman, E. Todorov, C. Cruz and S. Sevov, *Chem. Commun.*, 2000, 1213.
- 27 S. Ayyappan, G. Diaz de Delgado, G. Férey and C. N. R. Rao, *J. Chem. Soc., Dalton Trans.*, 1999, 2905.
- 28 N. Stock, G. D. Stucky and A. K. Cheetham, *Chem. Commun.*, 2000, 2277.
- 29 A. Cabeza, M. A. G. Aranda and S. Bruque, *J. Mater. Chem.*, 1998, **8**, 2479.
- 30 N. Stock, S. A. Frey, G. D. Stucky and A. K. Cheetham, *J. Chem. Soc., Dalton Trans.*, 2000, 4292.
- 31 H. G. Harvey, S. J. Teat and M. P. Attfield, *J. Mater. Chem.*, 2000, **10**, 2632.
- 32 (a) M. D. Poojary, D. Grohol and A. Clearfield, *Angew. Chem., Int. Ed. Engl.*, 1995, **34**, 1508; (b) M. A. G. Aranda, A. Cabeza, D. M. Poojary and A. Clearfield, *Inorg. Chem.*, 1996, **35**, 1468; (c) D. Grohol and Z. Clearfield, *J. Am. Chem. Soc.*, 1997, **119**, 9301; (d) J. A. Danis, W. H. Runde, B. Scott, J. Fettinger and B. Eichhorn, *Chem. Commun.*, 2001, 2378.
- 33 D. L. Lohse and S. C. Sevov, *Angew. Chem., Int. Ed. Engl.*, 1997, **36**, 1619.
- 34 D. M. Poojary, B. Zhang, P. Bellinghausen and A. Clearfield, *Inorg. Chem.*, 1996, **35**, 5254.
- 35 P.-A. Jaffrès, V. Caignaert and D. Villemin, *Chem. Commun.*, 1999, 1997.
- 36 (a) R. K. Cernik, W. Clegg, C. R. A. Catlow, G. Bushell-Wye, J. V. Flaherty, G. N. Greaves, I. Burrows, D. J. Tayler, S. J. Teat and M. Hamichi, *J. Synchrotron Radiat.*, 1997, **4**, 279; (b) W. Clegg, M. R. J. Elsegood, S. J. Teat, C. Redshaw and V. C. Gibson, *J. Chem. Soc., Dalton Trans.*, 1998, 3037.
- 37 G. M. Sheldrick, SHELXL-97, Program for Refinement of Crystal Structures, University of Göttingen, Germany, 1997.
- 38 L. J. Farrugia, WINGX, A Windows Program for Crystal Structure Analysis, University of Glasgow, UK, 1998.
- 39 A. C. Larson and R. B. Von Dreele, *GSAS, General Structure Analysis System, Report No. LA-UR-86-784*, Los Alamos National Laboratory, NM, USA, 1987.
- 40 D. Massiot, S. Drumel, P. Janvier, M. Bujoli-Doeuff and B. Bujoli, *Chem. Mater.*, 1997, **9**, 6.
- 41 N. B. Colthup, L. H. Daly and S. E. Wibberly, *Introduction to Infra Red and Raman Spectroscopy*, Academic Press Inc., San Diego, CA, 1990.
- 42 G. B. Hix, D. S. Wragg and R. E. Morris, *J. Chem. Soc., Dalton Trans.*, 1999, 3359.
- 43 R. Modi, G. B. Hix, M. Tremayne and E. J. MacLean, *New J. Chem.*, submitted.